Nonlinear Dyn
DOI 10.1007/s11071-007-9204-7

ORIGINAL ARTICLE

Bifurcation analysis of attitude control systems with switching-constrained actuators

A. Mesquita · E. L. Rempel · K. H. Kienitz

Received: 14 December 2005 / Accepted: 2 November 2006

Abstract On-off thrusters are frequently used as actuators for attitude control and are typically subject to switching constraints. In systems with switching actuators, different types of persistent motions may be found, and in the presence of model uncertainties, the occurrence of bifurcations in such systems can seriously affect performance. In this paper the nature of persistent motions in an attitude control system with actuators subject to switching-time restrictions is examined to provide useful information for control design in the presence of uncertainty. The main tools used are bifurcation diagrams, Poincaré maps and Lyapunov spectrum. Border-collision type bifurcations are characterized in this piecewise affine system, as well as unusual patterns of persistent motion. Multistability and complex-switching sequences are also observed, revealing the existence of motions with sensitive dependence on initial conditions.

Keywords Attitude control · Border-collision · Chaotic systems · Limit cycles · Quasi-periodic motion

A. Mesquita · K. H. Kienitz
Department of Systems and Control, Institute of Aeronautical Technology (ITA), CTA, 12228-900, São José dos Campos, SP, Brazil

E. L. Rempel (✉)
Department of Mathematics, Institute of Aeronautical Technology (ITA), CTA, 12228-900, São José dos Campos, SP, Brazil
e-mail: rempel@ita.br

1 Introduction

Launch and space vehicles may use on-off thrusters as actuators for attitude control. Examples of such systems are found in references [1–3]. Several types of on-off thrusters are available such as hydrazine, cold-gas and pulsed-plasma thrusters [4]. These thrusters produce discontinuous control actions and are affected by switching constraints. Common approaches for thruster activation logic are pulse modulation and direct control. The discussion of important aspects of pulse modulation usage in attitude control systems is found in [5, 6]. The present paper is concerned with direct control activation scenarios in which thruster switching constraints effectively impose limitations on dynamic actuator usage. In the literature such scenarios have not received much attention so far. As shown by Oliveira and Kienitz [3], non-conventional analysis/design problems may arise, because persistent system motions may not be of limit cycle type.

During recent research on the issue of limit cycle control for systems with minimally spaced switching-times, it was observed [7] that the optimal control parameter set, which guarantees minimum amplitude and minimum fuel consumption, lies on the frontier where the system bifurcates into nonperiodic persistent motions. Here the concern with the robustness of an optimal controller arises. In order to evaluate the system's robust performance, this paper is devoted to understanding these nonperiodic persistent motions.

In particular, its aim is to clarify how performance is affected by the emergence of these motions, and whether their amplitude or their appearance can be predicted. Hence, this paper presents the use of dynamical systems tools, such as bifurcation diagrams, Poincaré maps and Lyapunov spectrum, to characterize these motions.

In nonlinear systems, typical bifurcation phenomena include period-doubling cascades, saddle-node bifurcations and crises [8, 9]. Since this paper deals with a piecewise affine system subject to complex transition conditions, some unusual motions can be observed arising from periodic attractors by means of border-collision type bifurcations [10–12]. The stability of these motions is verified and their amplitudes are predicted. Moreover, the coexistence of multiple attractors for a given value of the control parameter (multistability) is observed, and chaotic attractors are found.

In Section 2, the roll control system being considered is described. Section 3 provides a global view of possible dynamics by means of Lyapunov spectrum analysis. Section 4 is devoted to the understanding of an attractor peculiar to systems with minimally spaced switching-times. In Section 5, the emergence of multistability is discussed. The final comments are given in Section 6.

2 Problem description

The problem description given here is akin to that in [3]. Consider a simple rigid body (e.g. satellite or rocket in the upper atmosphere) whose attitude angle ϕ is to be controlled using sets of small thrusters, which are on-off actuators with switching-time restrictions. A simplified representation of the system is shown in Fig. 1, where thrust F may assume final values $F_{\max}$, 0 or $-F_{\max}$.

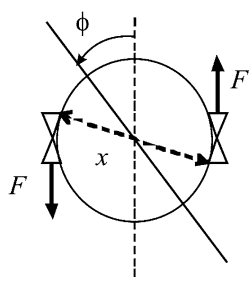

Fig. 1 Rigid body with set of thrusters

A body inertia $I_{xx} = 1500$ [kg m^2] is given. The small thruster actuators have delays and switching-time restrictions. Their characteristics are:

- Maximum absolute torque: $M = F_{\max} x = 308$ [Nm]
- Thrust build up dynamics given by the second order transfer function: $H(s) = \frac{86.8^2}{(s+86.8)^2}$, where s is a complex variable.
- Switching-time restrictions:
  - Minimum duration of pulses: $t_{\text{on}} = 100$ [ms]
  - Minimum rest between successive pulses of the same sign: $t_{\text{s}} = 50$ [ms]
  - Minimum rest between pulses of different sign: $t_{\text{off}} = 500$ [ms]

The typical requirement for the controlled system is that initial conditions and attitude perturbations shall asymptotically die away into a "well behaved" limit cycle. For the purpose of achieving appropriate performance, a tachometric feedback law and a first order compensator $C(s)$, having a zero at z and a pole at p, are added to the loop, resulting in the controlled system represented in Fig. 2.

The transfer function of the first order compensator is $C(s) = \frac{s-z}{s-p}$.

The "actuators" block of Fig. 2 can be decomposed into two parts: the first one containing switching actuators and the second one containing linear second order dynamics which models thrust build up. In practice, actuator delays may vary during the operation of the system. Their value may depend on several parameters. Thus the model is affected by uncertainty. Such uncertainty will not be considered here. All the gains in the system are rearranged to the output of the switching actuators block. Since the controller is linear, these gains affect only the amplitude of the response.

In summary, this system can be completely described by means of the discrete state variable $m = \{1; 2; 3; 4\} = \{F > 0; F = 0 \text{ after } F > 0; F < 0; F = 0 \text{ after } F < 0\}$ and the continuous state variable $y(t) = [\phi(t) \;\; d\phi(t)/dt \;\; I_{xx}^{-1} e(t) \;\; I_{xx}^{-1} de(t)/dt \;\; u(t) \;\; t_x(t)]^{\text{T}}$ where t is the independent time variable, $e(t)$ is the torque provided by actuators, $u(t)$ is the controller output, $t_x(t)$ is the time since the last transition, and superscript T stands for transpose.

The following is a state-space representation of the dynamics captured with the continuous state variable y:

$$\dot{y} = Ay + B \operatorname{sgn}(F)$$

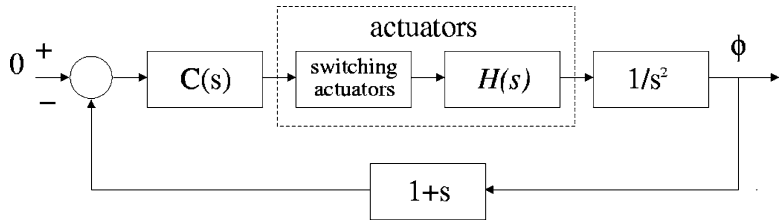

Fig. 2 Block diagram of the controlled system

$$A = \begin{bmatrix} 0 & 1 & 0 & 0 & 0 \\ 0 & 0 & 1 & 0 & 0 \\ 0 & 0 & 0 & 1 & 0 \\ 0 & 0 & -a^2 & -2a & 0 \\ z & z-1 & -1 & 0 & p \end{bmatrix},$$

$$B = \begin{bmatrix} 0 \\ 0 \\ 0 \\ a^2 M / I_{xx} \\ 0 \end{bmatrix} \tag{1}$$

For simplicity, the sixth state is suppressed because it is not directly dependent on other states and only affects switching conditions.

According to relay systems theory, for appropriate values of p and z, symmetric single-switching limit cycle behavior should be expected. Necessary conditions to the existence of such behavior can be provided either by approximate or exact methods (see [13]). The above switching-time restrictions impose another condition, which states the existence of a maximum switching frequency:

$$f_{\max} = \frac{1}{2(t_{\text{on}} + t_{\text{off}})} \tag{2}$$

The goal of this contribution is to analyze the susceptible kinds of behavior when one of these conditions is reached and, then, clarify the possibilities of robust performance for controllers operating near the bifurcation frontier.

3 Lyapunov spectrum

The Lyapunov spectrum is one of the standard tools to investigate the behavior of dynamical systems [14]. The Lyapunov exponents measure the average rate of divergence between nearby solutions of a dynamical system, and are calculated herein with the procedure suggested by Müller in [15]. This method is well suited for the calculation of Lyapunov exponents in nonsmooth systems because it takes into account the divergence between neighboring trajectories before and after crossing the switching surface. In the present case, since a piecewise affine system is used, the exact solution of the variational equation, used to compute the Lyapunov exponents, is known between transitions. Thus, it is possible to establish transition matrices relating the evolution of variations along successive switching surfaces. These matrices depend only on the state at the time of transition, which can be obtained with very high precision using the exact solution calculated from the last transition point. In order to efficiently calculate the exponents, the renormalization procedure based on QR-decomposition proposed in reference [16] is employed.

Results are illustrated in Fig. 3, where the four largest exponents are plotted as a function of control parameters p and z. The initial conditions are $y(0) = [-0.02 \quad 0.02 \quad 0 \quad 0 \quad 0 \quad 0]^{\text{T}}$ and $m(0) = 1$. Five large regions can be distinguished: two regions of periodic motion where $\lambda_1 = 0$ and $\lambda_i < 0$ for $i > 1$; two regions where $\lambda_1 \approx \lambda_2 \approx 0$ and λ_3 is slightly negative; and one region where the largest exponent is positive.

An improved understanding of these regions can be achieved with aid of Fig. 4, where a section of the diagrams in Fig. 3 is compared with other diagrams. The bifurcation diagram in Fig. 4(a) presents the dynamics of ϕ discretized using a Poincaré section which corresponds to the entry of the system into the discrete state $m = 2$, namely, this is the value of ϕ when the actuator switches from positive to null output. Note that this value is very close to the local minima of $\phi(t)$. The diagram in Fig. 4(b) exhibits the power spectral density of $\phi(t)$ for a sample rate of 20 [Hz] (see spectral bifurcation diagrams in [17]). In Fig. 4(c), the diagram for Lyapunov exponents shows the existence of a limit cycle for $-10.0 < z < -7.4$.

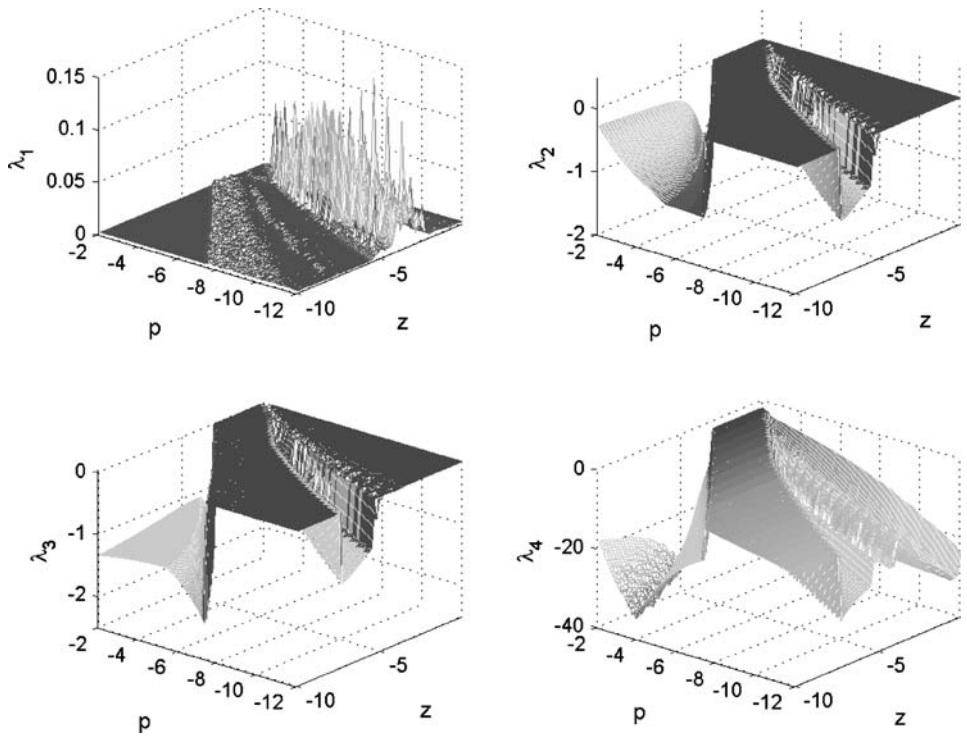

Fig. 3 Biparametric diagrams for the first four Lyapunov exponents

Moreover, as z is increased, diminishing the phase delay provided by the controller, diagrams 5(a) and 5(b) indicate an amplitude decrease and a frequency increase. However, as z enters the interval $(-7.4,\ -3.5)$, frequency attains the upper limit allowed by actuators restriction, $f_{\max} = 0.83$ [Hz], and a bifurcation occurs: very low frequencies gain considerable intensity and amplitude increases. Amplitude here is the maximum attained by a state variable in the attractor. This is an atypical motion that will be discussed in the next section. Further increase in z will cause a phase lead that brings the system "back" to periodic motion, which occurs for $-3.5 < z < -2.1$. In this region limit cycles with complex switching are observed. Instead of the simple sequence {1, 2, 3, 4} of m state transitions, complex sequences with time-asymmetric pulses occur, such as {1, 2, 1, 2, 3, 4, 3, 4} and {1, 2, 1, 2, 3, 4, 3, 4, 1, 2, 3, 4}. Beyond $z = -2.1$, switching becomes excessively complex, yielding very long periods and situations in which nearby trajectories diverge exponentially with time (chaotic trajectories with positive Lyapunov exponents).

4 Quasi-periodic-like behavior

This section is concerned with the nature of the non-periodic behavior that appears when actuators are requested to work on the limit defined by the switching restrictions. It is shown that the discretized map for the system presents an attractor given by a line segment of neutral fixed points and that outer orbits spiral towards this line segment without ever touching it. Additionally, the spiraling becomes slower at each turn, which suggests that the motion is the superposition of a periodic motion with frequency $f_{\max}$ and a second biased motion with constant amplitude and time-decreasing frequency. However, numerical results show that this second motion maintains a constant frequency band, which may be due to finite numerical precision. Actually, since a certain amount of sensor noise is always present in real systems, such numerical noise is not a concern in this case, and in simulations small random perturbations can even be added to the system, causing the attractor to be rapidly visited.

In this work, the composed motion is called *quasi-periodic-like* due to its similarities with quasiperiodic

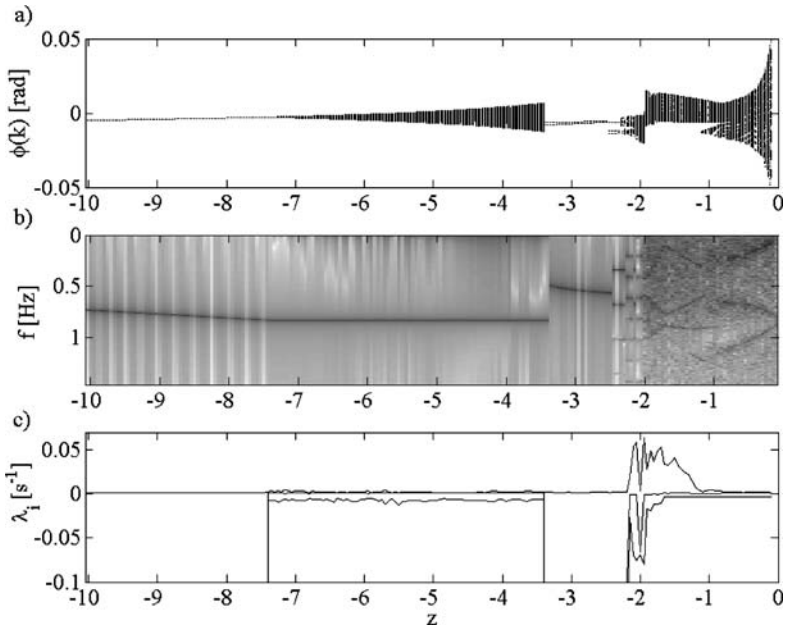

Fig. 4 A comparison of the bifurcation diagram for discretized ϕ (a), the spectral bifurcation diagram of ϕ (b), and the three largest Lyapunov exponents (c) for $p = -5.5$

motions [18]. Although one of the composing motions is not periodic, the maximum Lyapunov exponent is null and trajectories visit every neighborhood of an attractor that resembles a cylindrical hyper-surface in phase space.

Figure 5 illustrates how the bifurcation from periodic to quasi-periodic-like motion takes place in the vertex formed by the two switching surfaces. Initial conditions $y(0) = [0 \quad 0.02 \quad 0 \quad 0 \quad 0 \quad 0]^{\mathrm{T}}$ and $m(0) = 1$ are used. While in periodic motion (triangles) there are transitions to states 2 and 4 due to the crossing of $u = 0$, in quasi-periodic-like motion (black dots) these transitions occur because of the crossing of $t_x = 0.1$, which, unlike the periodic case, does not occur in only one point. Notice that in both cases symmetry is maintained.

In order to study this motion, let us define $Q = e^{2A(t_{\mathrm{on}}+t_{\mathrm{off}})}$ and $T = (I - e^{A(t_{\mathrm{on}}+t_{\mathrm{off}})}) \int_0^{t_{\mathrm{on}}} e^{A\tau} B d\tau$. Then, considering the case of the fastest allowed single switchings and using m as a subscript index to indicate the state of entry into mode m, it is possible to define the following discrete-time system:

$$y_2(k+1) = Q \cdot y_2(k) + T \tag{3}$$

Fixed points for this map will satisfy

$$(I - Q)\bar{y}_2 = T \tag{4}$$

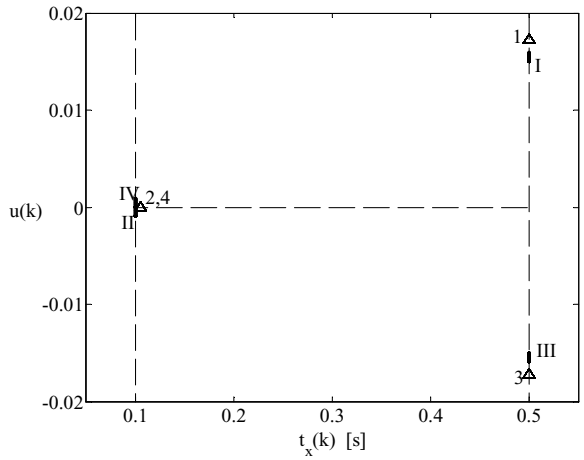

Fig. 5 Switching surfaces (*dashed lines*) and transition points for periodic (*triangles*; $p = -5.5$, $z = -7.6$) and quasi-periodic-like motions (*black dots*; $p = -5.5$, $z = -7.1$). Numbers indicate the sequence of discrete states

The matrix Q has the following structure

$$Q = \begin{bmatrix} 1 & 2(t_{\mathrm{on}} + t_{\mathrm{off}}) & q_{1,3} & q_{1,4} & 0 \\ 0 & 1 & q_{2,3} & q_{2,4} & 0 \\ 0 & 0 & q_{3,3} & q_{3,4} & 0 \\ 0 & 0 & q_{4,3} & q_{4,4} & 0 \\ \frac{z(e^{2p(t_{\mathrm{on}}+t_{\mathrm{off}})}-1)}{p} & q_{5,2} & q_{5,3} & q_{5,4} & e^{2p(t_{\mathrm{on}}+t_{\mathrm{off}})} \end{bmatrix} \tag{5}$$

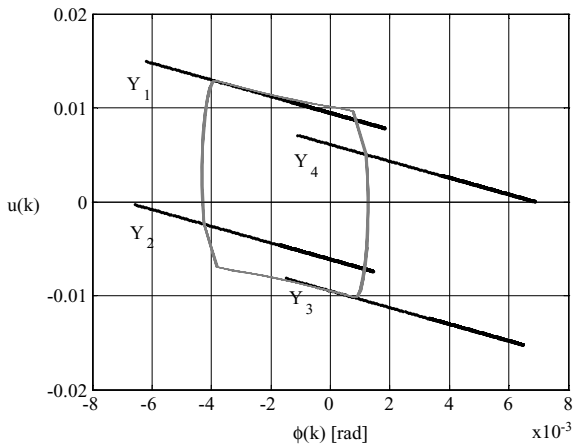

Fig. 6 Phase plot for quasi-periodic-like motion with $p = -5.5$, $z = -4.9$. Transition points are in black, while part of the associated continuous trajectory is plotted in gray

Due to the double integrator, A has two null eigenvalues and, consequently, Q has a double eigenvalue at 1. The corresponding eigenvector is $v = [\,1 \quad 0 \quad 0 \quad 0 \quad -z/p\,]^{\mathrm{T}}$. Thus, the set Y_2 of fixed points lies on the line $\bar{y}_2 + \alpha v$, where α is real and $\bar{y}_2$ is any given fixed point. Figure 6 presents a projection of sets Y_m and part of the associated continuous trajectory. The complete continuous attractor is the hypercylinder whose 'edges' lie on the line segments Y_m and whose base projection has the shape of the gray closed curve. A careful examination of the trajectory in the phase space reveals that the transition point $y_2(k)$ is indeed close to the local roll amplitude value. Switching conditions impose a limitation to the sets Y_m that can be noticed in Fig. 6: entry into mode $m = 2$ demands that $y_2(k)$ be such that $u_2(k) \leq 0$. Similarly, entry into mode $m = 4$ demands that $y_4(k)$ be such that $u_4(k) \geq 0$. In this way, one of the limits of Y_2 will be given by $y_2 = \bar{y}_2 + \alpha v$ such that $u_2 = 0$, the other limit will be given by the corresponding limit of Y_4. By rewriting Equation (7), one of the fixed points can be found:

$$\left(I - e^{2A(t_{\mathrm{on}}+t_{\mathrm{off}})}\right)\bar{y}_2 = \left(I - e^{A(t_{\mathrm{on}}+t_{\mathrm{off}})}\right)\int_0^{t_{\mathrm{on}}} e^{A\tau} B d\tau \quad (6)$$

It is easily seen that one possible solution is

$$\bar{y}_2 = \left(I + e^{A(t_{\mathrm{on}}+t_{\mathrm{off}})}\right)^{-1}\int_0^{t_{\mathrm{on}}} e^{A\tau} B d\tau \quad (7)$$

Then, considering the switching surface given by $Ny = u = 0$, where $N = [\,0 \quad 0 \quad 0 \quad 0 \quad 1\,]$, the first limit is the point

$$\bar{y}_2^1 = \bar{y}_2 - \frac{N\bar{y}_2}{Nv} v. \quad (8)$$

The second limit is $\bar{y}_2^2 = e^{A(t_{\mathrm{on}}+t_{\mathrm{off}})}\bar{y}_4^1 + \int_0^{t_{\mathrm{on}}} e^{A\tau} B d\tau$, but, because of symmetry, $\bar{y}_4^1 = -\bar{y}_2^1 = -\bar{y}_2 + \frac{N\bar{y}_2}{Nv} v$. Thus, substituting $\bar{y}_4^1$ and using Equation (7),

$$\bar{y}_2^2 = \bar{y}_2 + e^{A(t_{\mathrm{on}}+t_{\mathrm{off}})}\frac{N\bar{y}_2}{Nv} v = \bar{y}_2 + \frac{N\bar{y}_2}{Nv} v, \quad (9)$$

for v is an eigenvector of A. Predictions are compared to simulation in Fig. 7. Notice that, though a small amount of Gaussian white noise is added in the direction $w = [\,0 \quad 1 \quad 0 \quad 0 \quad 0\,]^{\mathrm{T}}$ right after each switching, there remained a few attractors not completely visited for the chosen integration time. The amplitude of the low frequency component is $y_b = -\frac{N\bar{y}_2}{Nv}$ and the amplitude of the component with frequency $f_{\max}$ is $y_a = \bar{y}_2$.

A similar analysis can be employed to find the bifurcation frontiers in the control parameters space for which this kind of motion disappears. These situations are such that $\bar{y}_2^1 = \bar{y}_2^2$ or $Ne^{At_{\mathrm{off}}}\bar{y}_2^1 = 0$, the latter case is that for which an intermediary switching becomes inevitable, for the states of entry in modes $m = 1$ or 3 have touched the other switching surface. In Fig. 6, it implies that line segments labeled Y_1 and Y_3 touch $u(k) = 0$.

With a little more algebra considering the matrix Q, it is possible to verify that $\bar{y}_2^1$ and $\bar{y}_2^2$ are hyperbolic functions of z. Thus, as long as the system is

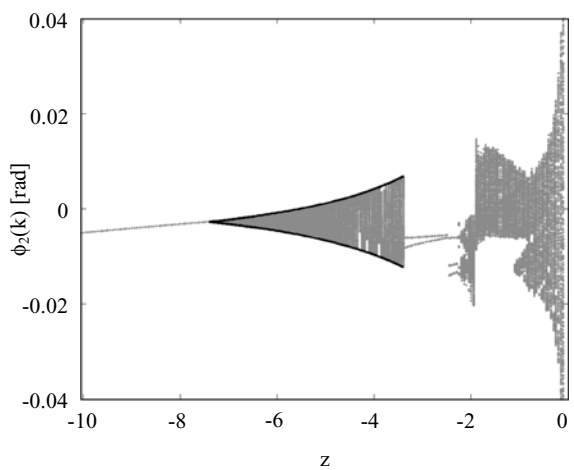

Fig. 7 Comparison of the predicted (*black lines*) and simulated (*gray dots*) limits of the quasi-periodic-like attractor

in quasi-periodic-like motion, phase leads cause an increase in roll amplitude, for this quantity is closely related to $\bar{y}_2^1$.

In view of the structure of matrix Q, disturbances of the fixed points in directions v or w must remain unmodified along iterations. Disturbances in direction w, however, cause directly proportional disturbances in direction v. Thus, disturbed orbits will follow lines parallel to v until they violate the fastest switching hypothesis. To understand what occurs when this hypothesis is about to be violated, suppose there is a negative disturbance of a fixed point in direction w. Then, the orbit will consist of negative fixed increments in direction v, which will make $u_2(k)$ increase. A moment will come when $u_2(k) > 0$. Thus, the minimum time for switching is reached but u is still positive; consequently, there will be a delay in switching. Since actuators will be set on longer than usual, switching will occur with an increased value of $d\phi/dt$. Thus, at each entry into state 2, $d\phi/dt$ will increase until it crosses the equilibrium value: $d\bar{\phi}_2/dt$. Then, the disturbance in w direction will be positive and the orbit will now follow the positive direction of v.

Figure 8 illustrates the sequence above. The arrows indicate the direction followed by the trajectory, starting with the long arrow at the bottom of the figure. In a first moment, $d\phi/dt$ is far below the equilibrium value (dashed line). That is why u suffers large increments. As previously mentioned, a delay causes the line $u = 0$ to be attained with an increased value of $d\phi/dt$, but still below the equilibrium value. The next point will be beyond, but closer to this same value. Now, u is being incremented by small amounts. Afterwards, the same routine is repeated for $y_4(k)$. The moment at which $u_4(k)$ crosses the axis is seen in Fig. 8 when the orbit becomes even closer to the equilibrium value.

The answer for how fast and whether disturbances disappear is given by the Lyapunov spectrum. Figures 4 and 5 show that there are two null Lyapunov exponents and a third exponent is very close to zero, but negative. One of the null exponents is related to disturbances along a periodic orbit. The second one is related to disturbances along v direction. The third exponent results from the fact that disturbances in w direction remain constant until the orbit crosses the switching surface, which happens more and more seldom as time goes by. In this way, disturbances in w direction have a very slow decay. The next section presents evidences of a similar spiraling motion for which disturbances in w direction

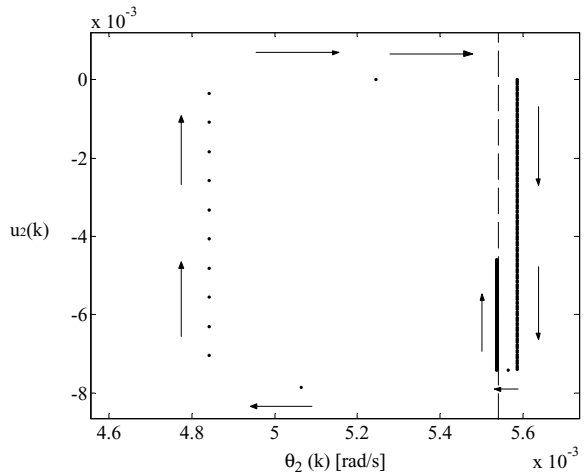

Fig. 8 Phase plot for transition points in quasi-periodic-like motion ($p = -5.5$, $z = -4.9$) in the neighborhood of the set of fixed points (*dashed line*)

do not decay. Trajectories performing quasi-periodic-like motion just reach the cylinder base and turn back immediately, which represents nonsmoothness in the low frequency component.

5 Multistability

The previous two sections presented results obtained from a single initial condition. Other choices of initial condition show the coexistence of multiple attractors for some parameters. In the range of parameter values considered in this work, the single-switching periodic motion seems to be a global attractor. Hence, for apparently any combination of control parameters where a single-switching periodic motion is found, it is the only attractor present in the phase space. On the other hand, quasi-periodic-like motion is not necessarily a global attractor. For $p = -5.5$, it is globally attractive only for z in the range $(-7.4, -3.5)$. For z in the range $(-3.5, -2.5)$, a quasi-periodic-like motion and a double-switching periodic motion with $\{m\} = \{1, 2, 1, 2, 3, 4, 3, 4\}$ coexist. A projection of the attractors for these two motions is plotted in Fig. 9. From this figure it can be seen that the double-switching periodic motion presents larger rate amplitude than the quasi-periodic-like motion. On the other hand, unlike the quasi-periodic-like motion, it does not present any bias. The transverse section of the basins of attraction depicted in Fig. 10 illustrates the complex way in which they are connected. The basin of the periodic attractor

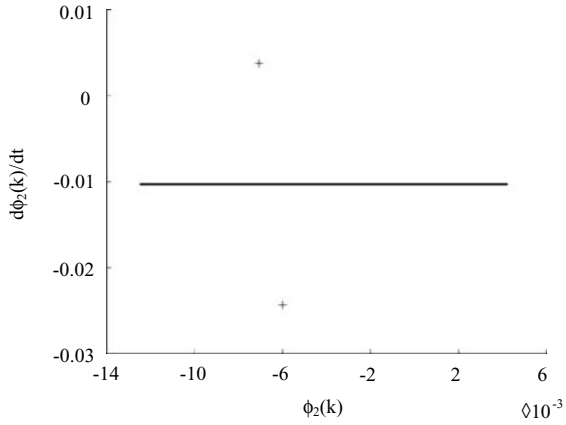

Fig. 9 Phase plot projection for transition points of the quasi-periodic-like attractor (*solid line*) and the double-switching periodic attractor (*crosses*) for $p = -5.5$, $z = -3.3$

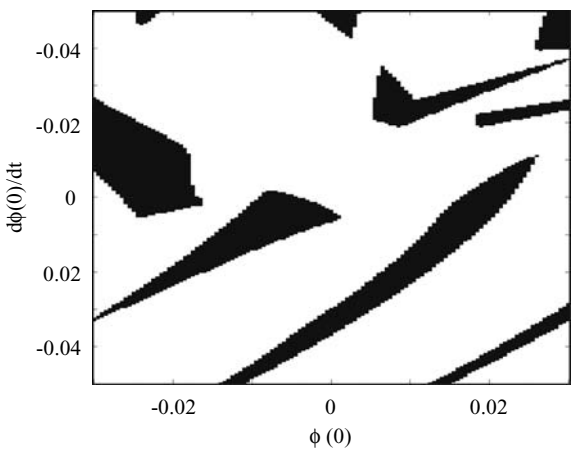

Fig. 10 Transverse section of the basins of attraction of the quasi-periodic-like attractor (*white*) and the double-switching periodic attractor (*black*). Other initial conditions are zero, $m(0) = 1$ and $p = -5.5$, $z = -3.3$

(black regions) grows larger as z approaches -2.5, a value at which the quasi-periodic-like attractor and its basin of attraction disappear due to collision of Y_1 and Y_3 with $u = 0$.

The abrupt change of the Lyapunov exponents at $z = -3.5$ is a signature of the grazing of the double-switching periodic attractor with a switching surface, which can be verified from Fig. 11, where the periodic attractor is tangent to the switching surface at point C for $z = -3.5$. A small decrement in z causes the destruction of the periodic attractor and the tangency point C. On the other hand, by increasing z this periodic attractor bifurcates into a quasi-periodic-like motion when another collision with a switching surface

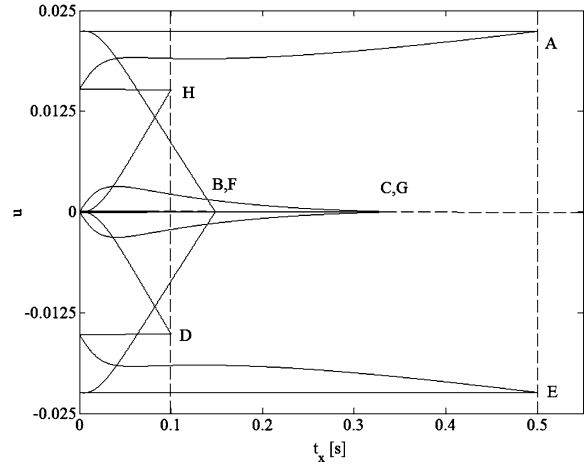

Fig. 11 Projection of the double-switching periodic attractor (*solid lines*) near the bifurcation at $p = -5.5$, $z = -3.5$. The dashed lines indicate the switching surfaces and the letters enumerate switching points

takes place at $z = -2.4$. In this new bifurcation, points B and F of Fig. 11 cross the vertex of the switching surface ($t_x = 0.1$, $u = 0$), which implies a delay in the switching of a non-restrained periodic motion. There is a crucial difference between the above-mentioned bifurcations. While in the first one the switching point suddenly disappears, in the second one the switching is only delayed, distorting the attractor and increasing its dimension. Therefore, we conclude that this system is subject to two distinct types of border collision bifurcations: one causing the appearance/disappearance of switching points, and a second one causing the scattering of switching points over $t_x = 0.1$.

There are procedures based on Tsypkin's method [3] that allow the *prediction* of the complex switching periodic motions. However, those methods become computationally too complex as switching possibilities grow. Hence, this work is limited to the detection of these motions, which are listed in Table 1. The notation 2 (λ_1, d_f, k) indicates that there is a pair of symmetric attractors with largest Lyapunov exponent λ_1, Lyapunov dimension d_f and k entries into the same mode by cycle. It is important to stress that periodic attractors (0, 1, k) are not always turned into quasi-periodic-like ones (0, 3, k) as z is increased. Take, for instance, the bifurcation of 2 (0, 1, 3), for $z = -2.4$, into a pair of chaotic attractors 2 (0.016, 3, 3), for $z = -2.2$. Finally, we stress that all these complex motions are disadvantageous from the control point of view, since they possess amplitudes far away from the minimum one, as shown

Table 1 Summary of observed attractors

$z(p=-5.5)$	Coexisting attractors (λ_1, d_f, k)[a]
−7.5	(0,1,1)
−7.4	(0,2,1)
−3.3	(0,1,2), (0,2,1)
−2.5	(0,1,2), 2 (0,1,3)
−2.4	(0,3,2), 2 (0,1,3)
−2.2	(0,3,1), (0,3,2), 2 (0.016,3,3), 2 (0.06,2.75,4), 2 (0,1,5)
−2.1	(0,3,2), 2 (0.02,3,3), 2 (0.05,2.8,5), 2 (0.03,2.11,7)
−2.0	2 (0,1,12), 2 (0,1,4), 2 (0.055,2.8,5)
−1.9	2 (0.02,3,?)[b], (0,3,4), 2 (0,3,12), (0,3,18)
−1.7	(0,3,16), (0,3,?), (0.05,3,?), (0,3,?)

[a] d_f is the Lyapunov dimension of the attractor and k is the number of transitions to a given mode at each cycle

[b] There is not a periodic sequence of mode transitions

in Fig. 7. Therefore, only single-switching periodic and quasi-periodic-like motions are interesting for control and other motions should be suppressed.

6 Concluding remarks

This paper presented and characterized the different possibilities of dynamic behavior in an attitude control system with time-constrained actuators. The goal of this study was to provide useful information for control design in the presence of uncertainties, since they seriously affect performance. A quasi-periodic-like behavior, the most relevant behavior other than the limit cycle, was explained and its amplitude was predicted. It was verified that the amplitude of this motion is more sensitive to control parameters than the limit cycle with simple switching. The consequences of complex-switching sequences in the actuators were also studied, revealing the existence of chaotic motions, with sensitive dependence on initial conditions. It was also concluded that such motions are disadvantageous from the control point of view, since they possess amplitudes far away from the minimum one. Therefore, only single-switching periodic and quasi-periodic-like motions are interesting for control and other motions should be suppressed.

Additional work is being carried out by the authors pursuing the analysis and synthesis of non-conservative robust performance controllers for the system considered. The results presented herein point to the design of a robust controller that allows operation both in periodic and quasi-periodic-like regions and avoids other motions.

Acknowledgements A. Mesquita and E. L. Rempel acknowledge financial support from Fundação de Amparo à Pesquisa do Estado de São Paulo (FAPESP).

References

1. Mendel, J.: On-off limit-cycle controllers for reaction-jet-controlled systems. IEEE Trans. Automatic Control **15**(3), 285–299 (1970)
2. Won, C.: Comparative study of various control methods for attitude control of a leo satellite. Aerosp. Sci. Technol. **3**(5), 323–333 (1999)
3. Oliveira, N.M., Kienitz, K.H.: Attitude controller design for a system using actuators with switching-time restrictions and delays. In: Proceedings of AIAA Guidance, Navigation, and Control Conference, Denver, CO, AIAA-2000-3967 (2000)
4. Antropov, N.N., Diakonov, G.A., Kazeev, M.N., Khodnenko, V.P., Kim, V., Popov, G.A., Pokryshkin, A.I.: Pulsed plasma thrusters for spacecraft attitude and orbit control system. In: Proceedings of the 26th International Propulsion Conference, Kitakyushu, Japan, October 17–21, pp. 1129–1135 (1999)
5. Avanzini, G., de Matteis, G.: Bifurcation analysis of attitude dynamics in rigid spacecraft with switching control logics. J. Guid. Control Dyn. **24**(5), 953–959 (2001)
6. Kienitz, K.H., Bals, J.: Pulse modulation for attitude control with thrusters subject to switching restrictions. Aerosp. Sci. Technol. **9**(7), 635–640 (2005)
7. Mesquita, A.R., Kienitz, K.H.: Persistent motion and chaos in attitude control with switching actuators. In: Proceedings of 16th IFAC World Congress, Prague, July 4–8, Conference CD-rom, paper Th-A03-TP/15 (2005)
8. Grebogi, C., Ott, E., Yorke, J.A.: Crises, sudden changes in chaotic attractors, and transient chaos. Physica D **7**(1–3), 181–200 (1983)
9. Rempel, E.L., Chian, A.C.-L.: Intermittency induced by attractor-merging crisis in the Kuramoto-Sivashinsky equation. Phys. Rev. E **71**(1), 016203 (2005)
10. Nusse, H.E., Ott, E., Yorke, J.A.: Border-collision bifurcations: an explanation for observed bifurcation phenomena. Phys. Rev. E **49**(2), 1073–1076 (1994)
11. Banerjee, S., Ranjan, P., Grebogi, C.: Bifurcation in two-dimensional piecewise smooth maps – theory and applications in switching circuits. IEEE Trans. Circuits Syst. I **47**(5), 633–643 (2000)
12. Zhusubaliyev, Zh.T., Soukhoterin, E.A., Mosekilde, E.: Border-collision bifurcations on a two-dimensional torus. Chaos Solitons Fractals **13**(9), 1889–1915 (2002)

13. Gille, J. Ch., Decaulne, P., Pélegrin, M.: Méthodes D'Étude des Systèmes Asservis Non Linéaires. Dunod, Paris, France (1967)
14. Alligood, K.T., Sauer, T.D., Yorke, J.A.: Chaos: An Introduction to Dynamical Systems. Springer-Verlag, New York (1996)
15. Müller, P.: Calculation of Lyapunov exponents for dynamic systems with discontinuities. Chaos Solitons Fractals **5**(9), 1671–1681 (1995)
16. Eckmann, J.-P., Ruelle, D.: Ergodic theory of chaos and strange attractors. Rev. Mod. Phys. **57**(3), 617–656 (1985)
17. Orrell, D., Smith, L.: Visualising bifurcations in high dimensional systems: the spectral bifurcation diagram. Int. J. Bif. Chaos **13**(10), 3015–3027 (2003)
18. Moser, J.: On the theory of quasi-periodic motions. SIAM Rev. **8**(2), 145–172 (1966)